Interference of Ca^{2+} with the proliferation of SCCOHT-1 and ovarian adenocarcinoma cells

ANNA OTTE, FINN RAUPRICH, JULIANE VON DER OHE, PETER HILLEMANNS and RALF HASS

Biochemistry and Tumor Biology Laboratory, Department of Obstetrics and Gynecology, Hannover Medical School, Hannover, Germany

Received April 14, 2014; Accepted May 27, 2014

DOI: 10.3892/ijo.2014.2518

Abstract. A recently established cellular model for the rare small cell carcinoma of the ovary hypercalcemic type (SCCOHT-1) was characterized in comparison to ovarian adenocarcinoma cells (NIH:OVCAR-3 and SK-OV-3). The different cancer populations exhibited a common sensitivity in acidic pH milieu and a continuous proliferation in alkaline medium of pH 8.0-9.0. In the presence of elevated Ca^{2+} concentrations, the ovarian cancer cells demonstrated a progressively reduced proliferation within 72 h in contrast to other tumor types such as breast cancer cells. This significant growth inhibition was calcium-specific since the proliferation was unaffected after culture of the ovarian cancer cells in the presence of similar concentrations of other cations. The Ca^{2+} effects on the ovarian cancer cells were associated with marked differences in the activation of intracellular signaling pathways including enhanced phosphorylation of the p42/44 MAP kinase (Thr202/Tyr204). Further analysis of the signaling pathway revealed a significantly enhanced Ca^{2+}-dependent and p42/44 MAP kinase activation-mediated prostaglandin E2 (PGE2) production in SK-OV-3 and SCCOHT-1 and to a lesser extent in NIH:OVCAR-3 cells. Vice versa, exogenous PGE2 did not affect the proliferative capacity of the ovarian cancer cells and inhibition of the Ca^{2+}-mediated MAP kinase activation did not abolish the Ca^{2+}-mediated cytotoxicity. Collectively, these data suggest that multiple pathways are activated by exogenous Ca^{2+} in the different ovarian cancer cells, including a specific MAP kinase signaling cascade with subsequent PGE2 production and a parallel pathway for the induction of cell death.

Correspondence to: Professor Ralf Hass, Biochemistry and Tumor Biology Laboratory, Gynecology Research Unit, Department of Gynecology and Obstetrics, Hannover Medical University, Carl-Neuberg-Str. 1, D-30625 Hannover, Germany
E-mail: hass.ralf@mh-hannover.de

Key words: small cell carcinoma of the ovary hypercalcemic type, ovarian cancer, tumor growth, Ca^{2+}-signaling, cell cycle, prostaglandin E2 production

Introduction

Ovarian cancer still represents one of the most lethal gynecologic malignancies. Within this type of gynecological cancer the small cell ovarian carcinoma of the hypercalcemic type (SCCOHT) is defined as a rare form of an aggressive ovarian tumor predominantly affecting young women between ages of 13 to 35 which is mostly associated with paraendocrine hypercalcemia (1-3). Following the initial histopathological evaluation of several clinical cases, the SCCOHT has been classified as a separate pathological entity (2). Recent studies revealed a mutation in the *SMARCA4* gene as a potential marker for the SCCOHT (4-6).

The SCCOHT tumor disease is associated with poor prognosis and appears different and clearly distinguishable from other ovarian cancer types such as ovarian epithelial tumors and ovarian germ cell tumors (7). Initial immunohistochemical analysis of the SCCOHT postulated a germ cell-derived tumor (8). Another study reported SCCOHT as an epithelial-like originating tumor (3). In fact, some cells stained positive for epithelial cell markers, however, the intermediate filament protein vimentin predominantly associated with cells of a mesenchymal phenotype has been identified in the majority of cells in the SCCOHT (9). Further investigations using additional genetic analysis of SCCOHT tumor specimen suggested a heterogeneous tumor entity but did not confirm a germ cell-derived or an epithelial cell-derived tumor origin (9-11). The heterogeneity of these data may be explained in part by the rare and limited tumor material from patients. Considering these controversial reports, the histogenesis of SCCOHT and the mechanism of the development and physiological role of an accompanying hypercalcemia still remain unclear. Likewise, reasonable approaches for a sufficient (chemo)therapeutic management to treat SCCOHT patients are completely unknown. Although a multi-modality platform is suggested including surgery followed by chemotherapy and radiotherapy (12,13), only very few patients survived longer than the following two years (14-17).

Recently, we developed a cellular model for the SCCOHT and the resulting SCCOHT-1 tumor cells were derived from a primary culture of biopsy material from a 31-year-old patient with recurrent SCCOHT. *In vivo* studies with these primary cells substantiated a SCCOHT phenotype with histopathological similarities between the mouse xenograft-developed

tumors and the original patient tumor. Moreover, development of SCCOHT-1-induced tumor xenografts displayed an accompanying hypercalcemia in NOD/scid mice with serum calcium levels above 3.5 mmol/l (1).

Using this unique cellular model, we examined in the present study the effects of exogenous calcium representing a hypercalcemia on SCCOHT-1 in comparison to established human ovarian adenocarcinoma cell lines including NIH:OVCAR-3 and SK-OV-3 cells. Moreover, different calcium-mediated signaling pathways were analysed in these ovarian cancer cells, which may be supportive in search of an appropriate therapeutic approach, particularly in SCCOHT.

Materials and methods

Cell culture

Primary human SCCOHT-1 cells. SCCOHT-1 cells were derived as a spontaneous, permanently growing primary culture from a tumor biopsy after surgery of a 31-year-old patient with recurrent SCCOHT (1). Informed written consent was obtained from the patient for the use of this material and the study was approved by the Ethics Committee of Hannover Medical School, Project #3916, June 15, 2005. The SCCOHT-1 cells were cultured in RPMI-1640 supplemented with 1 or 10% (v/v) fetal calf serum, 100 U/ml L-glutamine, 100 U/ml penicillin and 100 μg/ml streptomycin. The tissue culture was performed at 37˚C in a humidified atmosphere of 5% (v/v) CO_2 and the medium was changed at intervals of 3 to 4 days. For subculture, the cells were centrifuged (320 g/6 min) and resuspended in growth medium and the proliferative capacity at various conditions and the population doublings in parallel to the cell viability during culture was determined in a hemocytometer using the trypan blue exclusion test. In an alternative fluorescence-based proliferation assay the SCCOHT-1 cells have been transduced with a 3rd generation lentiviral SIN vector containing the eGFP gene (SCCOHT-1^{GFP}) as previously described for these cells (1).

Human ovarian adenocarcinoma cell lines. Human NIH:OVCAR-3 ovarian cancer cells (ATCC® #HTB-161™) were commercially obtained in passage 76 (P76) from the Institute for Applied Cell Culture (IAZ), Munich, Germany. The SK-OV-3 ovarian cancer cells (ATCC® #HTB-77™) were commercially obtained in P25 from the ATCC, Manassas, VA, USA. These ovarian adenocarcinoma cell lines were originally established from the malignant ascites of a patient with progressive adenocarcinoma of the ovary, respectively. The cells were cultivated at about 1,750 cells/cm^2 in RPMI-1640 supplemented with 1 or 10% (v/v) fetal calf serum, 100 U/ml L-glutamine, 100 U/ml penicillin and 100 μg/ml streptomycin. Subculture was performed by trypsin/EDTA (Biochrom GmbH, Berlin, Germany) treatment for 5 min at 37˚C. For the experiments NIH:OVCAR-3 cells were used in P86 to P118 and SK-OV-3 cells were used in P37 to P39. For fluorescence measurement in an appropriate proliferation assay the NIH:OVCAR-3 as well as the SK-OV-3 cells were also transduced with a eGFP gene vector (NIH:OVCAR-3^{GFP} and SK-OV-3^{GFP}) similar to SCCOHT-1^{GFP} cells.

Human breast cancer cell line. Human MDA-MB-231 breast cancer cells (MDA) were obtained from the ATCC (#HTB-26). This cell line was analyzed in a short tandem repeat (STR)-based authentication by the Institute for Legal Medicine at the University Hospital Schleswig-Holstein as recently documented (18). MDA cells were cultivated at about 1,500 cells/cm^2 in Leibovitz's L-15-medium (Invitrogen) with 10% (v/v) FCS, 2 mM L-glutamin and 1 mM penicillin/streptomycin. For fluorescence measurement MDA-MB-231^{GFP} cells were also generated after transduction with the eGFP gene vector.

Cell line authentication. Authentication of SCCOHT-1, NIH:OVCAR-3, SK-OV-3, and MDA-MB-231 cells was performed by short tandem repeat (STR) fragment analysis using the GenomeLab human STR primer set (Beckman Coulter Inc., Fullerton, CA, USA). Following DNA isolation of the cell lines and amplification by polymerase chain reaction (PCR) with the STR primer set, the appropriate PCR products were sequenced in the CEQ8000 Genetic Analysis System (Beckman Coulter) using the GenomeLab DNA size standard kit-600 (Beckman Coulter). Comparison of the sequencing results from SCCOHT-1 were similar to the original SCCOHT patient cells cultured in our lab. Moreover, the NIH:OVCAR-3, SK-OV-3 and MDA-MB-231 cell lines demonstrated a similar STR pattern according to the STR database provided by the Deutsche Sammlung von Mikroorganismen und Zellkulturen (DSMZ, Braunschweig, Germany) for these cell lines.

Proliferation and cell cycle analysis

For fluorescence measurement the different eGFP-transduced ovarian cancer populations were cultured in flat bottom 96-well plates (Nunc/ThermoFischer, Roskilde, Denmark) and incubated with 1.6, 3.2 and 6.4 mM Ca^{2+}, respectively, for 24 to 72 h. At different time points, the medium was removed and the cells were lysed with 5% (w/v) sodium dodecylsulfate (SDS). Thereafter, the fluorescence intensities of GFP in the cell homogenate which corresponded to the appropriate cell number of ovarian cancer cells, were measured at excitation 485 nm/emission 520 nm using the Fluoroscan Ascent Fl (Thermo Fisher Scientific) fluorescence plate reader.

To substantiate these results in an alternative assay, wild-type ovarian cancer populations were incubated similarly with 1.6, 3.2 and 6.4 mM Ca^{2+}, respectively, for 24 to 72 h and the cells were counted at the appropriate time points in a hemocytometer following trypan blue staining.

The cell cycle analysis was performed as described previously (19) using untreated compared to 1.6 mM Ca^{2+}- and 6.4 mM Ca^{2+}-stimulated SCCOHT-1^{GFP}, NIH:OVCAR-3^{GFP} and SK-OV-3^{GFP} ovarian cancer cells after 48 h. Briefly, $5x10^5$ cells were fixed in 70% (v/v) ice-cold ethanol at 4˚C for 24 h. Thereafter, the fixed cells were stained with CyStain DNA 2 step kit (Partec GmbH, Münster, Germany) and filtered through a 50 μm filter. The samples were then analyzed in a Galaxy flow cytometer (Partec) using the MultiCycle cell cycle software (Phoenix Flow Systems Inc., San Diego, CA, USA).

Immunoblot analysis

Following culture of SCCOHT-1^{GFP} cells in culture medium with 1% FCS, untreated control cells and Ca^{2+}-stimulated cells were washed three times in ice-cold PBS and lysed in a reswelling buffer containing 8 M urea (Carl Roth GmbH Co KG, Karlsruhe, Germany), 1% CHAPS (3-[(3-cholamidopropyl) dimethylammonio]-1-propanesulfonate) (Carl Roth GmbH

Co KG), 0.5% (v/v) pharmalyte 3-10 (GE Healthcare Europe GmbH, Freiburg, Germany), 0.002% (w/v) bromophenol blue (Serva Electrophoresis GmbH, Heidelberg, Germany) and freshly prepared 0.4% (w/v) dithiothreitol (DTT) (Carl Roth GmbH Co KG). Protein concentration was adjusted using the colorimetric BCA-assay (Perbio Science Deutschland, Bonn, Germany), subjected to SDS-polyacrylamide gel electrophoresis and transferred to a Hybond C Extra Nitrocellulose membrane (GE Healthcare Life Science). The membranes were blocked with PBS containing 5% FCS and 0.05% Tween-20 (PBS/Tween). After washing four times with PBS/Tween, the membranes were incubated with the primary antibodies (polyclonal anti-phospho-p44/42 MAPK$^{Thr202/Tyr204}$ (Cell Signaling Technology Inc.); polyclonal anti-Stim-1 (clone D88E10; Cell Signaling Technology Inc.); polyclonal anti-IP3 receptor (clone D53A5; Cell Signaling Technology Inc.); monoclonal anti-GAPDH (clone 6C5, Santa Cruz Biotechnology, Santa Cruz, CA, USA) at 4˚C overnight. Thereafter, the membranes were washed four times with PBS/Tween and incubated with the appropriate horseradish peroxidase-conjugated secondary antibody (all from Santa Cruz Biotechnology) for 1 h/25˚C. The membranes were washed with PBS/Tween and visualized by autoradiography using the ECL-detection kit (GE Healthcare Europe GmbH).

Prostaglandin E2 (PGE2) ELISA

SCCOHT-1^{WT}, SK-OV-3^{WT} and NIH:OVCAR-3^{WT} cells were seeded in 24-well plates at 10^6 cells/well (Nunc/ThermoFischer, Roskilde, Denmark) with 500 μl culture medium per well. In comparison to untreated control cells, the populations were stimulated with 1.6, 3.2 and 6.4 mM Ca^{2+}, respectively, in the absence or presence of a 1-h pre-incubation with 50 μM of the MAP kinase inhibitor PD98059 (Cell Signaling Technology Inc.). The conditioned medium was collected after 12 and 24 h, respectively, and centrifuged at 1,000 rpm/10 min. Thereafter, 50 μl aliquots of the supernatant were applied to the appropriate PGE2 measurements which were performed in an ELISA system according to the manufacturer's recommendation (R&D Systems Ltd., Abingdon, UK).

Results

Proliferation. All three ovarian cancer cell types exhibited sensitivity for an acidic culture milieu and continued maximal proliferation in alkaline medium of approximately pH 9.0 (Fig. 2). The proliferative capacity of SCCOHT-1 and NIH:OVCAR-3 cells was progressively inhibited by about 80% at pH 6.0 within 72 h (n=5) whereas SK-OV-3 cells demonstrated more stability with a growth reduction of about 30% (n=6). At pH 10.0 the proliferation progressively declined by 59±4% (n=5) in SCCOHT-1 cells after 72 h. A higher sensitivity with 80±2% (n=5) was observed in NIH:OVCAR-3 cells at pH 10.0 after 72 h and SK-OV-3 cells revealed 41±6% (n=5) growth inhibition at similar conditions (Fig. 1).

According to the hypercalcemia associated with SCCOHT, exogenous stimulation with calcium was tested and revealed a significant growth inhibition in all three ovarian carcinoma cell types in a concentration- and time-dependent manner. Whereas the culture medium constitutively contained about 0.8 mM Ca^{2+} and Mg^{2+} during steady-state culture conditions,

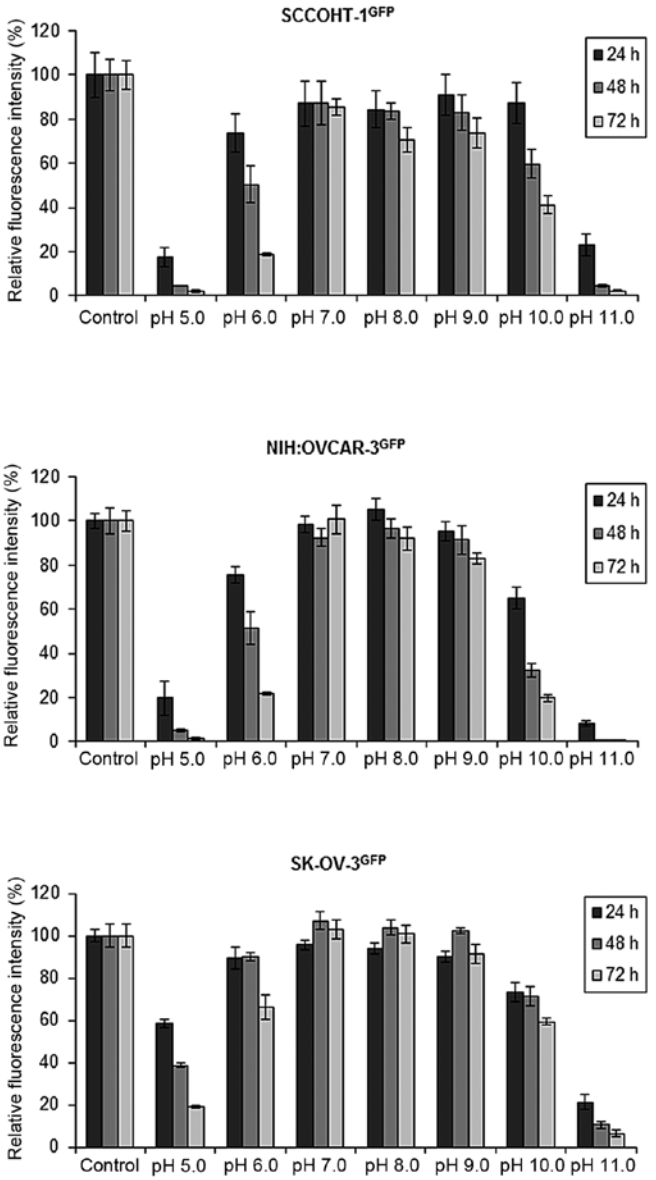

Figure 1. The proliferation of different ovarian cancer cell types (SCCOHT-1^{GFP}, NIH:OVCAR-3^{GFP} and SK-OV-3^{GFP} cells) was evaluated in a fluorescence-based assay under various pH conditions in the range of pH 5.0 to pH 11.0 as compared to control cells cultured at pH 7.4 for 24 to 72 h. Every 24 h, the medium was exchanged with newly established pH following appropriate adjustments by HCl or NaOH, respectively. Data represent the mean ± SD (n=5).

the proliferative capacity of SK-OV-3 cells after exogenous addition of 1.6 mM Ca^{2+} up to 6.4 mM Ca^{2+} was progressively reduced to 17.8±6.2% (n=10) within 72 h. These growth-inhibitory effects of 6.4 mM Ca^{2+} were even more pronounced in SCCOHT-1 with growth reduction down to 11.4±5.0% (n=9) and were maximal in NIH:OVCAR-3 cells reaching only 3.8±0.5% (n=10) of proliferative capacity after 72 h as compared to control cells in normal culture medium (Fig. 2A). In contrast to these significant growth-inhibitory effects of Ca^{2+}, incubation of the three ovarian carcinoma cell populations with 6.4 mM Mg^{2+} demonstrated little if any effect on the cell growth and remained at a normal growth rate of approximately 100% within 72 h (Fig. 2A). Moreover, culture of the breast cancer cell line MDA-MB-231 in the

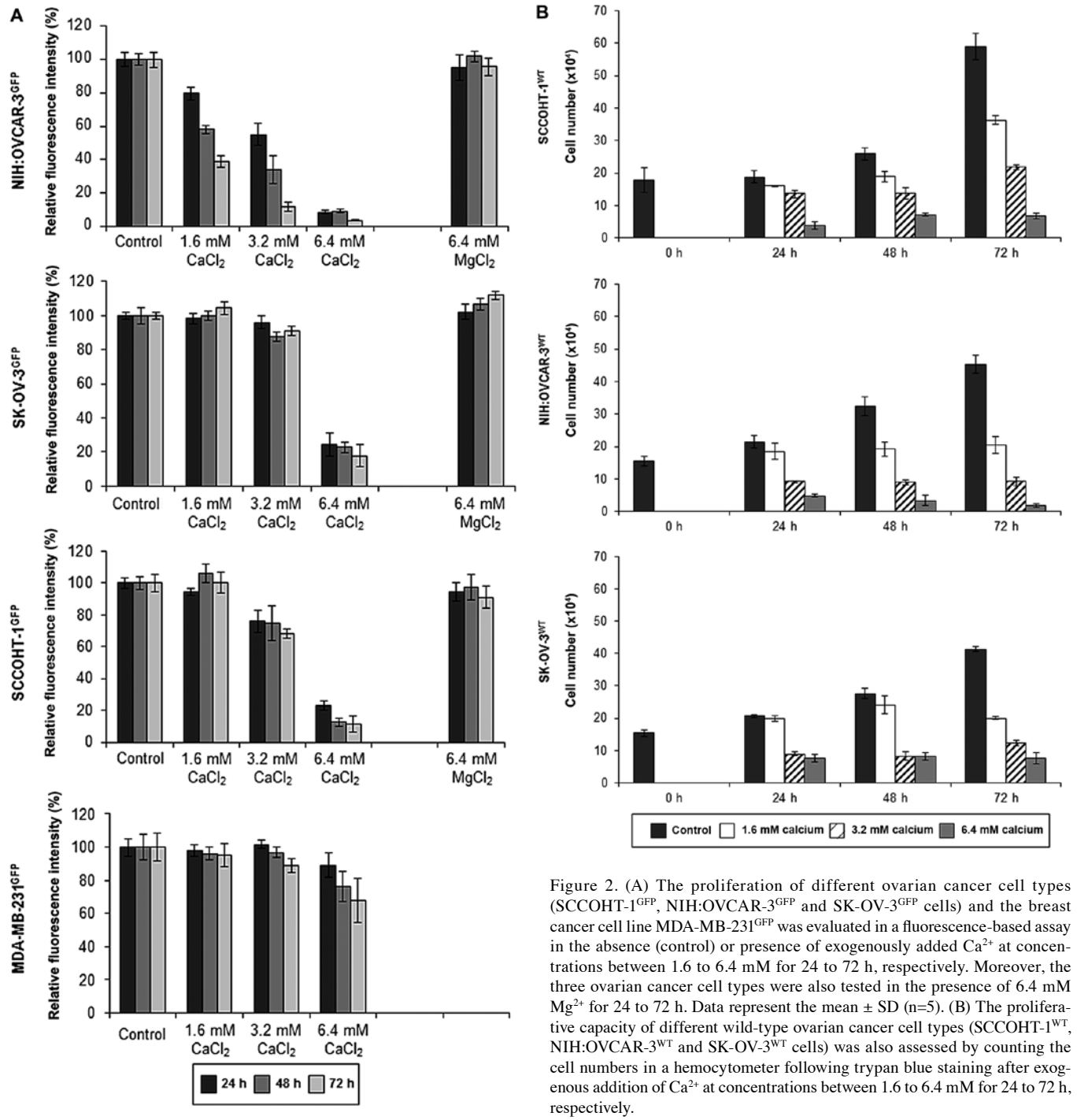

Figure 2. (A) The proliferation of different ovarian cancer cell types (SCCOHT-1^{GFP}, NIH:OVCAR-3^{GFP} and SK-OV-3^{GFP} cells) and the breast cancer cell line MDA-MB-231^{GFP} was evaluated in a fluorescence-based assay in the absence (control) or presence of exogenously added Ca^{2+} at concentrations between 1.6 to 6.4 mM for 24 to 72 h, respectively. Moreover, the three ovarian cancer cell types were also tested in the presence of 6.4 mM Mg^{2+} for 24 to 72 h. Data represent the mean ± SD (n=5). (B) The proliferative capacity of different wild-type ovarian cancer cell types (SCCOHT-1^{WT}, NIH:OVCAR-3^{WT} and SK-OV-3^{WT} cells) was also assessed by counting the cell numbers in a hemocytometer following trypan blue staining after exogenous addition of Ca^{2+} at concentrations between 1.6 to 6.4 mM for 24 to 72 h, respectively.

presence of 6.4 mM Ca^{2+} was associated with a growth rate of 68.1±13.2% (n=6) compared to a control culture after 72 h (Fig. 2A). Similar results of a marked Ca^{2+}-mediated concentration- and time-dependent growth inhibition were also obtained with the appropriate wild-type ovarian cancer cell populations by cell counting in a trypan blue exclusion assay (Fig. 2B). The results from the proliferation assays were also accompanied by appropriate morphological changes. Whereas the different ovarian cancer cell types demonstrated their typical morphology in phase contrast microscopy of the control cultures together with a GFP expression of the lentiviral eGPF-transduced cultures, a significant cell death with rounded and granulated cell bodies was observed in NIH:OVCAR-3^{GFP} cells following exposure to 6.4 mM Ca^{2+} for 72 h (Fig. 3, upper panel). Moreover, little if any fluorescence was detectable anymore in NIH:OVCAR-3^{GFP} cells. Only few GFP-expressing viable cells remained in the SCCOHT-1^{GFP} culture after incubation with 6.4 mM Ca^{2+} for 72 h (Fig. 3, middle panel). SK-OV-3^{GFP} cells also exhibited a significant granulation after incubation with exogenous Ca^{2+} with some more GFP-positive viable cells which substantiated the results of the proliferation assay (Fig. 3, lower panel).

Cell cycle analysis revealed a significant arrest of SCCOHT-1^{GFP} cells in the G_2 phase after 48 h in the presence of 1.6 mM Ca^{2+}. An elevation to 6.4 mM Ca^{2+} was associated with increased cell death by an accumulation of SCCOHT-1^{GFP}

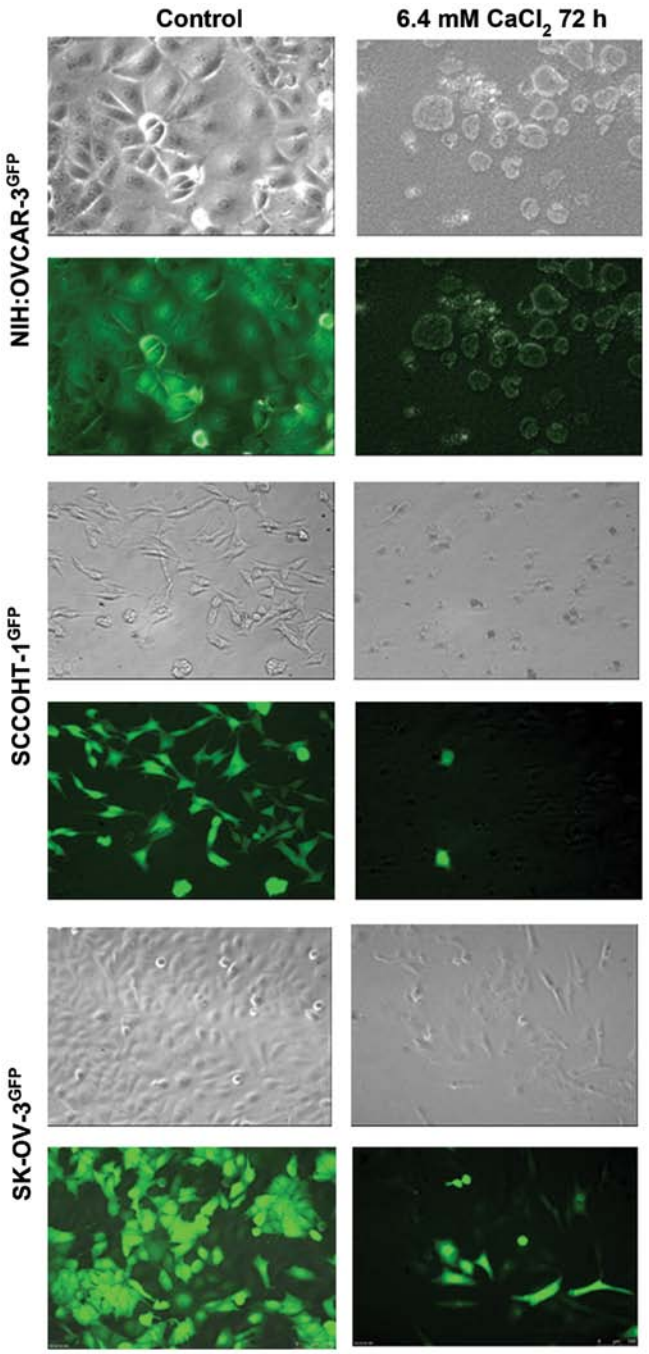

Figure 3. The morphology of NIH:OVCAR-3^{GFP} (upper panel), SCCOHT-1^{GFP} (middle panel) and SK-OV-3^{GFP} (lower panel) cells was documented by phase contrast (grey) and fluorescence microscopy (green) in untreated control cells and after incubation in the presence of 6.4 mM Ca^{2+} for 72 h.

cells in the subG$_1$ phase. Similar findings were observed in 6.4 mM Ca^{2+}-exposed NIH:OVCAR-3^{GFP} cells with significantly elevated levels of cells in the subG$_1$ phase after 48 h whereas the cell cycle of the lesser Ca^{2+}-sensitive SK-OV-3^{GFP} cells still remained unaltered (Fig. 4).

Together, these findings suggested an optimal growth of the different ovarian cancer cells in a neutral to alkaline pH range whereby enhanced exogenous Ca^{2+} significantly reduced the proliferative capacity and tumor cell viability. Western blot analysis was performed to further investigate specific signaling effects of Ca^{2+} in the different ovarian cancer cells. Exposure to 1.6 mM Ca^{2+} revealed a marked appearance of phosphorylated p42/44 MAP kinase (Thr202/Tyr204) within 2 h in SCCOHT-1 cells and this phosphorylation signal sustained for at least 24 h (Fig. 5A). A constitutive p42/44 MAP kinase phosphorylation in NIH:OVCAR-3 and SK-OV-3 cells was initially reduced by exogenous Ca^{2+} and significantly increased after 4 to 8 h before this signal was markedly reduced again within 24 h (Fig. 5B and C). Ca^{2+}-sensitizing proteins were also investigated, including stromal interaction molecule-1 (Stim-1) which determines differences in [Ca^{2+}] in the endoplasmic reticulum and can oscillate for stimulatory interactions with the ORAI1 calcium ion channels to the plasma membrane (20). The Stim-1 expression was enhanced between 1 and 2 h of 1.6 mM Ca^{2+} treatment of SCCOHT-1 cells (Fig. 5A), whereas little, if any, different Stim-1 protein levels were observed in NIH:OVCAR-3 and SK-OV-3 cells until a decrease was observed after 24 h (Fig. 5B and C). With respect to the IP3 receptor which releases Ca^{2+} from endoplasmic storage compartments upon phospholipase C-mediated PI-breakdown and inositol trisphosphate generation, there was only marginal if any change in the IP3 receptor protein levels following Ca^{2+} stimulation of the ovarian cancer cells. The unaltered GAPDH expression served as loading control (Fig. 5A).

Ca^{2+}-mediated phosphorylation of p42/44 MAP kinase (Thr202/Tyr204) was associated with enhanced PGE2 production in the ovarian cancer cells. Thus, stimulation of SK-OV-3 cells with increasing [Ca^{2+}] between 1.6 and 6.4 mM exhibited progressively increasing PGE2 release after 12 h, which was significantly further elevated after 24 h following Ca^{2+} stimulation (Fig. 6A). Moreover, pre-treatment with the p42/44 MAP kinase inhibitor PD98059 completely abolished even the highest levels of Ca^{2+}-mediated PGE2 production (Fig. 6A). Similar results were obtained in SCCOHT-1 cells with 40.4±24.1 pg/ml PGE2 after 1.6 mM Ca^{2+} and 232.5±37.9 pg/ml PGE2 after 6.4 mM Ca^{2+} stimulation for 12 h. Likewise, NIH:OVCAR-3 cells produced 41.2±0.1 pg/ml PGE2 after 1.6 mM Ca^{2+} and 48.4±0.1 pg/ml PGE2 after 6.4 mM Ca^{2+} incubation within 24 h whereas non-stimulated control cells displayed 12.1±0.1 pg/ml PGE2 and the PGE2 concentrations in the presence of the MAP kinase inhibitor PD98059 were below detection limit. To test any potential growth-inhibitory effects of PGE2 on the different ovarian cancer populations, SCCOHT-1, NIH:OVCAR-3 and SK-OV-3 cells were incubated with various PGE2 concentrations between 1 pg/ml to 10 ng/ml and revealed little if any effect on the proliferative capacity of the tumor cells (Fig. 6B). Together, these findings suggested that the Ca^{2+}-mediated p42/44 MAP kinase phosphorylation and subsequent stimulation of PGE2 production was independent of the Ca^{2+}-mediated growth inhibition. Indeed, this suggestion was substantiated by the MAP kinase inhibitor PD98059 which completely abolished the Ca^{2+}-mediated p42/44 MAP kinase phosphorylation in SCCOHT-1 cells (Fig. 7A). Moreover, MAP kinase inhibition did not demonstrate any effect on the increased G$_2$ arrest by 1.6 mM Ca^{2+} nor on the pronounced cell death of SCCOHT-1 cells in subG1 phase by 6.4 mM Ca^{2+} after 48 h similar to the results in Fig. 4 (Fig. 7B).

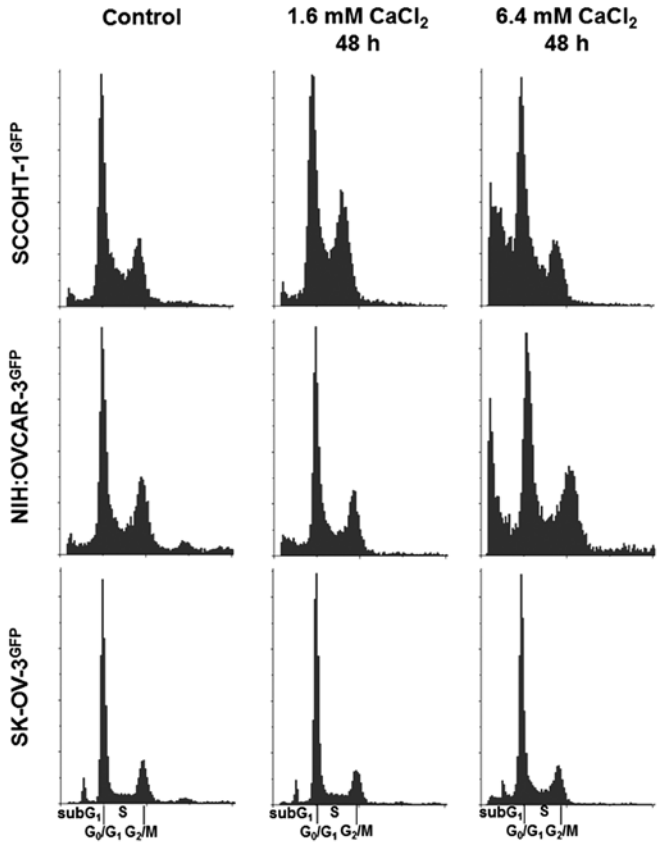

Figure 4. Cell cycle analysis was performed in SCCOHT-1^{GFP} (upper panel), NIH:OVCAR-3^{GFP} (middle panel) and SK-OV-3^{GFP} (lower panel) cells in the absence (control) or presence of exogenously added Ca^{2+} at concentrations of 1.6 and 6.4 mM for 48 h, respectively.

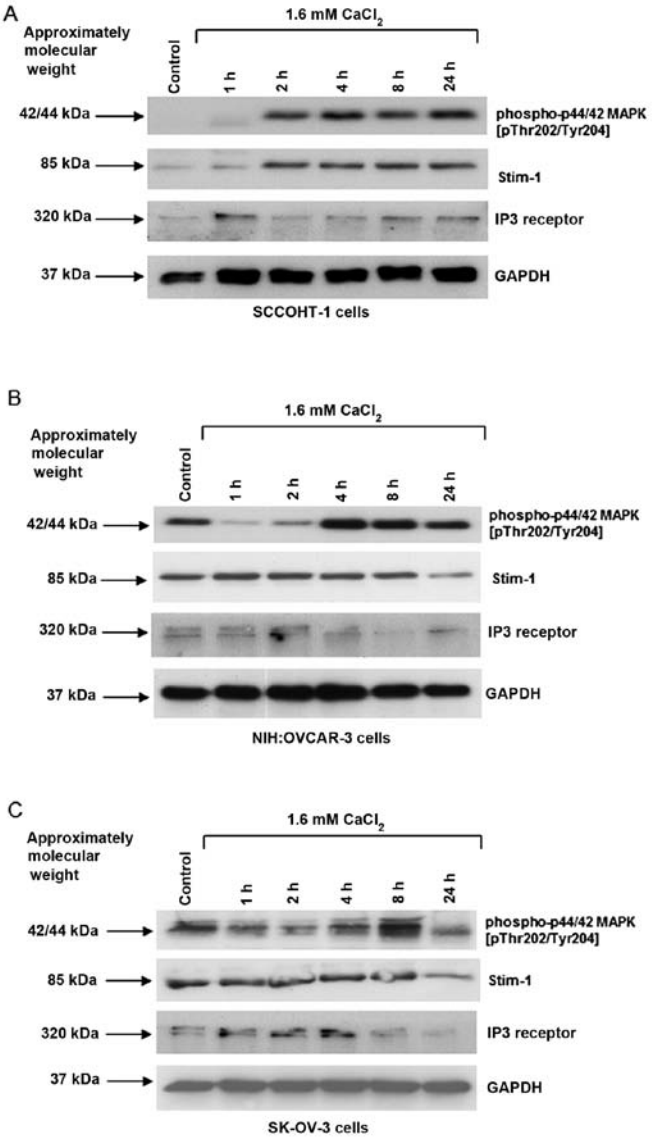

Figure 5. Western blot analysis was performed with proteins from (A) SCCOHT-1^{GFP}, (B) NIH:OVCAR-3^{GFP} and (C) SK-OV-3^{GFP} cells following incubation in the absence (control) or presence of 1.6 mM exogenously added Ca^{2+} for 1 h up to 24 h, respectively. The blots were incubated with the anti-phospho-p44/42 $MAPK^{Thr202/Tyr204}$, anti-Stim-1 and anti-IP3 receptor antibody, respectively. Protein levels of GAPDH served as a loading control.

Discussion

Ovarian cancer represents the predominant cause of gynecological cancer-related deaths affecting approximately 65,000 females in economically-developed countries in 2011 (21). As a rare form and special kind of ovarian cancer, the SCCOHT represents an aggressive tumor with poor prognosis and characteristics as compared to other ovarian carcinoma types remain unclear. The *in vitro* results in this study revealed common pH sensitivity in acidic milieu and continuous proliferation in neutral/low alkaline environment. Whereas young patients diagnosed with SCCOHT often present with a concomitant serum hypercalcemia, it was of interest to focus on calcium effects in ovarian cancer cells.

According to normal serum calcium levels of 2 to 2.5 mmol/l, hypercalcemia is considered as a mild type at concentrations between 2.5 to 3.0 mmol/l serum calcium and as a moderate type at concentrations between 3.0 to 3.5 mmol/l serum calcium. Patients with serum calcium levels above 3.5 mmol/l are diagnosed with a hypercalcemic crisis. Of interest, a recent study in a variety of ovarian cancer patients reports elevated blood calcium levels whereby $[Ca^{2+}]$ was proposed a potential predictive marker for ovarian cancer (22).

To test different levels of hypercalcemia *in vitro*, calcium concentrations of 1.6, 3.2 and 6.4 mmol/l were applied to the various ovarian cancer cells and revealed already significant growth-inhibitory effects between mild and moderate hypercalcemia. These growth-inhibitory effects were calcium-specific, since none of these results were obtained with similar concentrations of Mg^{2+} or further cations. Moreover, other tumor types such as breast cancer cells demonstrated much less responsiveness to high Ca^{2+} concentrations as compared to the different ovarian cancer cells. This calcium sensitivity of ovarian cancer cells suggested that elevated $[Ca^{2+}]$ is supportive for a therapeutic approach particularly in SCCOHT. Additional examination of these growth-inhibitory effects of high $[Ca^{2+}]$ *in vitro* demonstrated a morphological disintegration of the ovarian cancer cells. This was associated with increased cell death as revealed by cell cycle analysis. Interference with the calcium homeostasis can induce cell damage and eventually initiate cell death (23), whereby

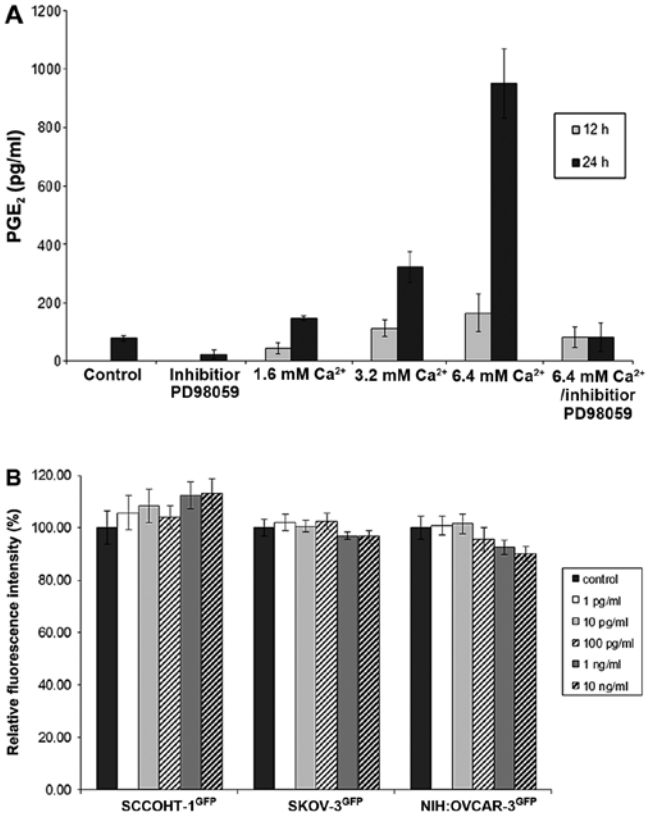

Figure 6. (A) The amount of released prostaglandin E2 (PGE2) was evaluated by ELISA in the supernatant of SK-OV-3^{WT} cells following stimulation in the absence (control) or exogenous addition of Ca^{2+} at concentrations between 1.6 to 6.4 mM for 12 and 24 h, respectively. Moreover, PGE2 levels were measured in the supernatant of control cells after incubation with 50 μM of the p44/42 MAPK inhibitor PD98059 for 24 h (inhibitor PD98059), and following stimulation of the cells with 6.4 mM Ca^{2+} in the presence of the MAPK inhibitor PD98059 for 12 and 24 h, respectively. Data represent the mean + SD (n=3). (B) The proliferation of different ovarian cancer cell types (SCCOHT-1^{GFP}, NIH:OVCAR-3^{GFP} and SK-OV-3^{GFP} cells) was evaluated in a fluorescence-based assay following stimulation of the different populations with various concentration of PGE2 between 1 pg/ml to 10 ng/ml for 72 h. Data represent the mean ± SD (n=5).

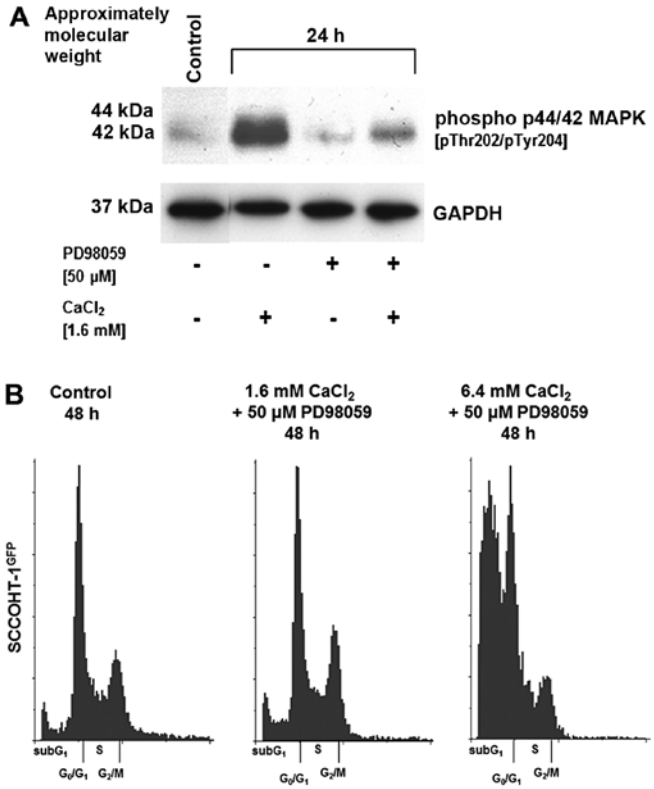

Figure 7. (A) Western blot analysis was performed for the anti-phospho-p44/42 MAPK$^{Thr202/Tyr204}$ protein levels in SCCOHT-1^{GFP} cells following incubation in the absence (control) or presence of 1.6 mM exogenously added Ca^{2+}, 50 μM of the p44/42 MAPK inhibitor PD98059 or both, 1.6 mM Ca^{2+} and 50 μM PD98059 for 24 h, respectively. Incubation of the blot with anti-GAPDH antibody served as a loading control. (B) Cell cycle analysis was performed in SCCOHT-1^{GFP} cells pre-incubated for 1 h with 50 μM of the p44/42 MAPK inhibitor PD98059 and further cultured in the absence (control) or presence of exogenously added Ca^{2+} at concentrations of 1.6 and 6.4 mM for 48 h, respectively.

recent studies proposed a process of programmed necrosis (necroptosis) upon cytosolic calcium accumulation in mouse xenografts of human neuroblastoma (24). These findings further substantiate our hypothesis that suitable chemotherapeutic compounds in combination with increased calcium levels contribute to an enhanced promotion of tumor cell death particularly in SCCOHT-1 cells. In this context, the hypercalcemia associated with SCCOHT may reflect a physiological anti-tumor response. However, due to a certain protection of the tumor cells within the tumor microenvironment and potential interactions with other cell types including immune cells and mesenchymal stem/stroma cells as documented for other tumor types such as breast cancer (18,25,26), the hypercalcemic effects achieve only a limited threshold and therefore, remain unresponsive and inefficient without further support to directly target the SCCOHT cancer cells.

At the molecular level, high [Ca^{2+}] was associated with increased activation/phosphorylation of the p42/p44 MAPK in the ovarian cancer cells. Activated p42/p44 MAPK can further relay phosphorylation signals to eventually stimulate phospholipase A2 (27). Upon cleavage of polyunsaturated fatty acids including arachidonic acid from the C2-position of membrane phospholipids by activated phospholipase A2, the elevated levels of arachidonic acid can be further metabolized via cyclooxygenase isoforms (COX-1, COX-2) into prostanoids and predominantly PGE2 (28,29). Indeed, the data obtained in the present study substantiated such a signaling pathway, whereby stimulation of the ovarian cancer cells with increasing calcium concentration resulted in appropriately increasing PGE2 production both, in a concentration- and time-dependent manner. Enhanced PGE2-synthesis accompanied by an increased expression of COX-1 and COX-2 has been documented in certain epithelial ovarian cancer (30) indicating potential metabolic alterations with the malignant transformation and progression. PGE2 can mediate suppressive effects via ligation to the E prostanoid receptors EP2 and EP4 followed by enhanced production of cyclic AMP. However, PGE2 binding to EP3 can also exert immune-stimulatory properties by decreasing cAMP levels. Therefore, PGE2-mediated immune-modulation by tumors can alter immune surveillance by re-educating the infiltrating inflammatory and immune cells to support tumorigenesis (31). Whereby no direct proliferative effects of PGE2 on the ovarian cancer cells were detectable, our work also demonstrated

that the calcium-mediated PGE2 production was p42/p44 MAPK-dependent since MAPK inhibition abolished the PGE2 production in the different ovarian cancer cells.

Together, increased calcium concentrations can specifically stimulate PGE2 production via p42/p44 MAPK activation and in parallel, contribute to the induction of cell death in ovarian cancer cells, whereby these calcium-mediated effects are relayed via different signaling pathways. Although the appearance of a serum hypercalcemia in SCCOHT patients and a variety of other ovarian cancer patient exhibit only a limited and insufficient threshold, the present findings indicate that elevated Ca^{2+} levels can enhance a physiological antitumor strategy for SCCOHT in support of a combined therapeutic approach against this rare but severe type of ovarian cancer.

Acknowledgements

This study was supported by a grant from the Niedersächsische Krebsgesellschaft e.V. to R.H.

References

1. Otte A, Gohring G, Steinemann D, *et al*: A tumor-derived population (SCCOHT-1) as cellular model for a small cell ovarian carcinoma of the hypercalcemic type. Int J Oncol 41: 765-775, 2012.
2. Dickersin GR, Kline IW and Scully RE: Small cell carcinoma of the ovary with hypercalcemia: a report of eleven cases. Cancer 49: 188-197, 1982.
3. Young RH, Oliva E and Scully RE: Small cell carcinoma of the hypercalcemic type in the ovary. Gynecol Oncol 57: 7-8, 1995.
4. Jelinic P, Mueller JJ, Olvera N, *et al*: Recurrent SMARCA4 mutations in small cell carcinoma of the ovary. Nat Genet 46: 424-426, 2014.
5. Witkowski L, Carrot-Zhang J, Albrecht S, *et al*: Germline and somatic SMARCA4 mutations characterize small cell carcinoma of the ovary, hypercalcemic type. Nat Genet 46: 438-443, 2014.
6. Ramos P, Karnezis AN, Craig DW, *et al*: Small cell carcinoma of the ovary, hypercalcemic type, displays frequent inactivating germline and somatic mutations in SMARCA4. Nat Genet 46: 427-429, 2014.
7. Scully RE: Atlas of Tumor Pathology: Tumors of the Ovary and Maldeveloped Gonads. Armed Forces Institute of Pathology, Washington, DC, 1979.
8. Ulbright TM, Roth LM, Stehman FB, Talerman A and Senekjian EK: Poorly differentiated (small cell) carcinoma of the ovary in young women: evidence supporting a germ cell origin. Hum Pathol 18: 175-184, 1987.
9. Aguirre P, Thor AD and Scully RE: Ovarian small cell carcinoma. Histogenetic considerations based on immunohistochemical and other findings. Am J Clin Pathol 92: 140-149, 1989.
10. Walt H, Hornung R, Fink D, *et al*: Hypercalcemic-type of small cell carcinoma of the ovary: characterization of a new tumor line. Anticancer Res 21: 3253-3259, 2001.
11. McCluggage WG, Oliva E, Connolly LE, McBride HA and Young RH: An immunohistochemical analysis of ovarian small cell carcinoma of hypercalcemic type. Int J Gynecol Pathol 23: 330-336, 2004.
12. Harrison ML, Hoskins P, du Bois A, *et al*: Small cell of the ovary, hypercalcemic type - analysis of combined experience and recommendation for management. A GCIG study. Gynecol Oncol 100: 233-238, 2006.
13. Shrimali RK, Correa PD and Reed NS: Dose-dense and dose-intense chemotherapy for small cell ovarian cancer: 2 cases and review of literature. Med Oncol 28: 766-770, 2011.
14. Benrubi GI, Pitel P and Lammert N: Small cell carcinoma of the ovary with hypercalcemia responsive to sequencing chemotherapy. South Med J 86: 247-248, 1993.
15. Reed WC: Small cell carcinoma of the ovary with hypercalcemia: report of a case of survival without recurrence 5 years after surgery and chemotherapy. Gynecol Oncol 56: 452-455, 1995.
16. Dykgraaf RH, de Jong D, van Veen M, Ewing-Graham PC, Helmerhorst TJ and van der Burg ME: Clinical management of ovarian small-cell carcinoma of the hypercalcemic type: a proposal for conservative surgery in an advanced stage of disease. Int J Gynecol Cancer 19: 348-353, 2009.
17. Barondeau J, Rodgers M, Braun L, Azarow K, Forouhar M and Faucette K: Small cell ovarian carcinoma: a rare, aggressive tumor masquerading as constipation in a teenager with a fatal outcome. J Pediatr Hematol Oncol 32: e139-e141, 2010.
18. Mandel K, Yang Y, Schambach A, Glage S, Otte A and Hass R: Mesenchymal stem cells directly interact with breast cancer cells and promote tumor cell growth in vitro and in vivo. Stem Cells Dev 22: 3114-3127, 2013.
19. Bertram C and Hass R: Cellular senescence of human mammary epithelial cells (HMEC) is associated with an altered MMP-7/HB-EGF signaling and increased formation of elastin-like structures. Mech Ageing Dev 130: 657-669, 2009.
20. Putney JW: Capacitative calcium entry: from concept to molecules. Immunol Rev 231: 10-22, 2009.
21. Jemal A, Bray F, Center MM, Ferlay J, Ward E and Forman D: Global cancer statistics. CA Cancer J Clin 61: 69-90, 2011.
22. Schwartz GG and Skinner HG: Prospective studies of total and ionized serum calcium in relation to incident and fatal ovarian cancer. Gynecol Oncol 129: 169-172, 2013.
23. Trump BF and Berezesky IK: Calcium-mediated cell injury and cell death. FASEB J 9: 219-228, 1995.
24. Nomura M, Ueno A, Saga K, Fukuzawa M and Kaneda Y: Accumulation of cytosolic calcium induces necroptotic cell death in human neuroblastoma. Cancer Res 74: 1056-1066, 2014.
25. Ungefroren H, Sebens S, Seidl D, Lehnert H and Hass R: Interaction of tumor cells with the microenvironment. Cell Commun Signal 9: 18, 2011.
26. Hass R and Otte A: Mesenchymal stem cells as all-round supporters in a normal and neoplastic microenvironment. Cell Commun Signal 10: 26, 2012.
27. Van Rossum GS, Klooster R, van den Bosch H, Verkleij AJ and Boonstra J: Phosphorylation of p42/44(MAPK) by various signal transduction pathways activates cytosolic phospholipase A(2) to variable degrees. J Biol Chem 276: 28976-28983, 2001.
28. Koehler L, Hass R, DeWitt DL, Resch K and Goppelt-Struebe M: Glucocorticoid-induced reduction of prostanoid synthesis in TPA-differentiated U937 cells is mainly due to a reduced cyclooxygenase activity. Biochem Pharmacol 40: 1307-1316, 1990.
29. Rehfeldt W, Hass R and Goppelt-Struebe M: Characterization of phospholipase A2 in monocytic cell lines. Functional and biochemical aspects of membrane association. Biochem J 276: 631-636, 1991.
30. Rask K, Zhu Y, Wang W, Hedin L and Sundfeldt K: Ovarian epithelial cancer: a role for PGE2-synthesis and signalling in malignant transformation and progression. Mol Cancer 5: 62, 2006.
31. Medeiros A, Peres-Buzalaf C, Fortino Verdan F and Serezani CH: Prostaglandin E2 and the suppression of phagocyte innate immune responses in different organs. Mediators Inflamm 2012: 327568, 2012.